HAL
open science

Prelamin A mediated recruitment of SUN1 to the nuclear envelope directs nuclear positioning in human muscle

Giovanna Lattanzi, Elisabetta Mattioli, Marta Columbaro, Cristina Capanni, Nadir Mario Maraldi, Vittoria Cenni, Katia Scotlandi, Maria Teresa Martino, Luciano Merlini, Stefano Squarzoni

To cite this version:

Giovanna Lattanzi, Elisabetta Mattioli, Marta Columbaro, Cristina Capanni, Nadir Mario Maraldi, et al.. Prelamin A mediated recruitment of SUN1 to the nuclear envelope directs nuclear positioning in human muscle. Cell Death and Differentiation, 2011, 10.1038/cdd.2010.183 . hal-00614318

HAL Id: hal-00614318

https://hal.science/hal-00614318v1

Submitted on 11 Aug 2011

HAL is a multi-disciplinary open access archive for the deposit and dissemination of scientific research documents, whether they are published or not. The documents may come from teaching and research institutions in France or abroad, or from public or private research centers.

L'archive ouverte pluridisciplinaire **HAL**, est destinée au dépôt et à la diffusion de documents scientifiques de niveau recherche, publiés ou non, émanant des établissements d'enseignement et de recherche français ou étrangers, des laboratoires publics ou privés.

Running title

SUN1/prelamin A interplay in human skeletal muscle

TITLE

Prelamin A mediated recruitment of SUN1 to the nuclear envelope directs nuclear positioning in human muscle

Elisabetta Mattioli[a], Marta Columbaro[b], Cristina Capanni[a], Nadir M. Maraldi[b], Vittoria Cenni[a], Katia Scotlandi[c], Maria Teresa Marino[c], Luciano Merlini[b], Stefano Squarzoni[a], Giovanna Lattanzi[a*].

[a]Institute for Molecular Genetics, IGM-CNR, Unit of Bologna I-40136 Bologna, Italy;

[b]Laboratory of Musculoskeletal Cell Biology, Istituto Ortopedico Rizzoli I-40136 Bologna, Italy

[c]Laboratory of Oncological Research, Istituto Ortopedico Rizzoli I-40136 Bologna, Italy

***Correspondence to**:

Dr. Giovanna Lattanzi

IGM-CNR, Unit of Bologna c/o IOR

Via di Barbiano 1/10

I-40136 Bologna Italy

TEL. +39-0516366394

FAX +39-051583593

E-mail: lattanzi@area.bo.cnr.it

giovanna.lattanzi@cnr.it

ABSTRACT

Lamin A is a nuclear lamina constituent expressed in differentiated cells. Mutations in the *LMNA* gene cause several diseases, including muscular dystrophy and cardiomyopathy. Among nuclear envelope partners of lamin A are SUN1 and SUN2, which mediate nucleo-cytoskeleton interactions critical to the anchorage of nuclei. In this study, we show that differentiating human myoblasts accumulate farnesylated prelamin A, which elicits upregulation and recruitment of SUN1 to the nuclear envelope and favors SUN2 enrichment at the nuclear poles. Indeed, impairment of prelamin A farnesylation alters SUN1 recruitment and SUN2 localization. Moreover, nuclear positioning in myotubes is severely affected in the absence of farnesylated prelamin A. Importantly, reduced prelamin A and SUN1 levels are observed in Emery-Dreifuss muscular dystrophy myoblasts, concomitant with altered myonuclear positioning. These results demonstrate that the interplay between SUN1 and farnesylated prelamin A contributes to nuclear positioning in human myofibers and may be implicated in pathogenetic mechanisms.

INTRODUCTION

Formation of multinucleated myotubes from cells committed towards myogenic differentiation is required to maintain muscle tissue homeostasis. Myotubes are formed through a two-step mechanism: primary myotubes are formed by fusion of lined-up myoblasts, while other committed cells are fused laterally to primary myotubes to form secondary myotubes (1). During this process, nuclei become regularly spaced and myonuclear domains are well defined in the cytoplasm. Noticeably, the mechanism regulating nuclear positioning in myotubes involves critical transcription factors such as NFATc (2) and FHL1 (3), cytoskeleton constituents including desmin (4) and tubulins (5) and an increasing number of nuclear envelope proteins such as nesprins (6), SUN1 and SUN2 (7).

SUN proteins are integral proteins of the nuclear envelope known to anchor nesprins to the nucleoskeleton (8, 9). SUN1 has been shown to form dimers and hetero-dimers with SUN2 and to reside in the inner nuclear membrane of mammalian cells, with its C-terminal moiety in the perinuclear space (10). SUN proteins have been reported to anchor centrosomes to centromere clusters (11, 12). Recent reports show that they play a role in skeletal muscle (7) and SUN2 has been involved in the proper positioning of nuclei at the human neuromuscular junctions and in mouse myofibers, a function affected by lamin A pathogenetic mutations (13). These data have provided increasing evidence of a functional link between the cytoskeleton and the nucleus potentially implicated in myogenic differentiation . However, partners regulating the dynamic behavior of SUNs and nesprins in the myoblast nuclear envelope have been elusive.

Recently, defective nuclear anchorage has been linked to mutations or absence of lamin A/C (13, 14)**.** Lamins A and C are major constituents of the nuclear lamina produced by alternative splicing from the *LMNA* gene. They have been implicated in various functions including nuclear stability, transcriptional control, cell cycle regulation, nucleo-cytoplasmic interplay, cellular signaling and heterochromatin dynamics (14-18). Although lamin A is ubiquitously expressed in differentiated tissues, a key role of lamin A in skeletal muscle is demonstrated by several published data showing its involvement in cell cycle exit (19), cellular signalling (20, 21), induction of muscle-specific genes (22-24) and nuclear positioning at the neuromuscular junctions (13). Mutations in the *LMNA* gene cause skeletal and cardiac muscle disorders in Emery-Dreifuss muscular dystrophy (EDMD) (25), limb-girdle muscular dystrophy type 1B (26) or dilated cardiomyopathy with conduction defect (27). Moreover, muscle atrophy or misfunctioning have been reported in progeroid disorders linked to lamin A mutations such as Hutchinson-Gilford progeria (28), Mandibuloacral dysplasia (29, 30) and atypical-Werner syndrome (31). These and other diseases caused by mutations in lamins or lamin-binding proteins are referred to as laminopathies or nuclear envelopathies.

In the context of lamin A-related disorders, prelamin A, the precursor protein of lamin A, has emerged as a key pathogenic factor (17). Newly translated prelamin A undergoes a rapid multi-step processing, which triggers formation of three intermediate products: full-length farnesylated prelamin A, cleaved farnesylated prelamin A and carboxymethylated farnesylated prelamin A. Proteolytic removal of the farnesylated C-terminus end is carried out by a specific endoprotease called ZMPSTE24 and yields mature lamin A (32, 33). A biological role of the lamin A precursor is also suggested by its modulation in normal cells, mostly during

differentiation. Prelamin A has been shown to influence chromatin dynamics, emerin localization, nuclear import of the transcription factor SREBP1 in adipocytes and early events of myoblast differentiation (22, 34-36).

In the reported study, we focused on prelamin A processing and SUN1 interplay in human muscle cells. We demonstrate that SUN1 is retained at the nuclear envelope of human muscle progenitors through farnesylated prelamin A-dependent mechanisms. In fact, impairment of prelamin A farnesylation abolishes SUN1 recruitment to myotube nuclei, leading to myonuclear clustering. Clustering of myonuclei also occurs in EDMD myotubes showing reduced prelamin A and SUN1 levels. On the other hand, increasing levels of farnesylated prelamin A and SUN1 in adult muscle are suggestive of a role of these proteins in muscle homeostasis.

RESULTS AND DISCUSSION

SUN1 and farnesylated prelamin A are recruited to the nuclear envelope in differentiated muscle cells

Bright staining of SUN1 was observed in cycling myoblasts, but it was considerably reduced in resting myoblasts (Fig. 1A arrowheads) and it started to increase in cells committed to differentiation (caveolin 3 positive mononucleated cells, Fig. 1A). Conversely, labeling of SUN2 was not significantly changed in myoblast subpopulations at any stage (Fig.1A). Unexpectedly, SUN1 fluorescence intensity was enhanced in myotubes, while SUN2 staining increased in a lower percentage of myotube nuclei (Fig. 1A). Moreover, farnesylated prelamin A was absent from cycling myoblasts, while it was detected in committed myoblasts and myotubes, throughout the differentiation process (Fig. 1 A). In fact, 1188-2 anti-prelamin A antibody, which selectively binds farnesylated prelamin A (37) (Fig. 1 B), brightly stained the nuclear envelope and, less intensely, the nucleoplasm, in all of the multinucleated cells (Fig. 1 A). Other anti-prelamin A antibodies, which were directed to non-farnesylated epitopes in the prelamin A C-terminus (Fig. 1 B), failed to stain prelamin A in human muscle cells, at any stage (Fig. 1 C-D). Although farnesylated prelamin A could not be detected in nuclear lysates, due to the low efficiency of 1188-2 antibody in Western blot analysis, the immunochemical analysis supported the finding that SUN1 levels were decreased in resting myoblasts, while they rose again in myotubes (Fig. 1E-F, statistically significant increase of SUN1 in differentiated cell cultures, $p < 0.05$). Intriguingly, a 200 kDa band, likely corresponding to a SUN1 dimer, was detected in myotubes, but not in cycling or resting cells (Fig. 1E) (10). SUN2 expression was not significantly changed at any stage in nuclear lysates (Fig.

1E-F). Thus, our results, in agreement with reported data (22, 38), showed modulation of SUN1 and prelamin A levels during myogenesis.

SUN2, farnesylated prelamin A and SUN1 at the nuclear poles and in tissues

Next, we compared the localization of prelamin A and SUN proteins at the nuclear envelope of human muscle cells (Fig. 2). Colocalization of farnesylated prelamin A and SUN1 was observed in committed myoblasts and myotubes (Fig. 2A). Moreover, the mean fluorescence intensity of SUN2, prelamin A and SUN1 was measured in cycling, resting cells or differentiate myoblasts (300 nuclei per sample). The statistical analysis reported in figure 2B shows parallel upregulation of proteins in myotubes. In depth evaluation of protein localization in committed myoblasts and myotubes allowed us to show that, while the nuclear envelope protein emerin was evenly distributed in the nuclear membrane, SUN2 was concentrated at one or both the nuclear poles in about 60% of nuclei (Figure 2C-G). Farnesylated prelamin A was localized along the nuclear rim, but it was enriched at the nuclear poles in more than 60% of myotube nuclei (Fig. C-G). SUN1 was enriched at one side of the nuclear envelope, possibly corresponding to the site of attachment of the microtubule-organizing center (MTOC), in 35% of myotube nuclei (Fig. 2C-G). However, double immunofluorescence staining of FLAG-tagged farnesylated prelamin A and SUN2 showed co-localization at the nuclear poles (Fig. 2D). Both statistical analysis (Fig. 2 E) and examination of fluorescence intensity profile of the nuclear envelope (Fig. 2 G), confirmed polarization of SUN2, prelamin A and SUN1 in committed myoblasts and myotubes. The nuclear poles are the extremities of the major axis of the cell nucleus. They anchor cytoskeletal proteins implicated in nuclear movement (39, 40). Thus, data here reported hint at a key role of SUNs and farnesylated prelamin A in myonuclear positioning.

Localization of SUN proteins and prelamin A was also investigated in mature muscle. We observed SUN1, SUN2 and prelamin A labeling at the nuclear envelope of myofibers (Fig. 2H). The nuclear envelope constituents were also detected at the myotendinous junctions, identified by integrin beta 1D labeling (Fig. 2H), and at the neuromuscular junctions, labeled by alpha-bungarotoxin staining of acetylcoline receptors (Fig. 2H). Colocalization of SUN2, farnesylated prelamin A and SUN1 was observed in the same nuclei in serial muscle sections (Fig. 2H).

Overexpression of farnesylated prelamin A enhances SUN1 levels

Because it had been reported that recruitment of SUN1 to the nuclear envelope is mediated by prelamin A (41, 42), while we had shown that prelamin A levels are increased in differentiating mouse muscle (22), we investigated a mechanistic role of prelamin A in SUN1 recruitment in human myoblasts.

To evaluate prelamin A effects on SUN1 recruitment, we transfected HEK293 cells with prelamin A constructs. Wild-type prelamin A (LA-WT), which is processed to mature lamin A, LA-C661M prelamin A, which cannot be farnesylated, LA-L647R prelamin A, which is farnesylated but cannot undergo endoproteolysis (Fig. 3A), were overexpressed in nuclei. In HEK293 cells, overexpression of farnesylated prelamin A caused a striking increase of SUN1 and SUN2 staining at the nuclear envelope (Fig. 3B). It is noteworthy that basal levels of SUN1 and SUN2 fluorescence intensity were very low in HEK293 cells (Fig. 3B). Western blot analysis confirmed that overexpression of prelamin A causes upregulation of SUN1 (Fig. 3C). SUN2 levels were not affected, as determined by Western blot analysis (Fig. 3C), suggesting an increased accessibility of native SUN2 to IF antibody labeling in transfected HEK293 cells. Moreover, we found that farnesylated prelamin A, but not other prelamin A constructs, co-immunoprecipitated SUN1 in vivo (Fig. 3C). However, a double

prelamin A mutant (LA-L647R/R527P), carrying the pathogenetic R527P *LMNA* mutation that hinders SUN1 binding (43), failed to bind prelamin A (Fig. 3C), suggesting that some other interaction in the lamin A/C domain is required to stabilize prelamin A binding. Conversely, SUN2 and emerin bound any prelamin A form with the same affinity (Fig. 3C). To evaluate possible transcriptional regulation of SUN1 by farnesylated prelamin A, we analyzed SUN1 transcripts. The real-time RT-PCR analysis showed three-fold upregulation of SUN1 expression in cells overexpressing farnesylated prelamin A, but downregulation of transcripts in the presence of non-farnesylated prelamin A (Fig. 3D). We further hypothesized that prelamin A binding might stabilize SUN1 at the nuclear envelope in transfected HEK293 cells. Treatment of untransfected cells with the proteasome inhibitor MG132 or the lysosome inhibitor chloroquine increased SUN1 levels indicating that degradation of SUN1 does occur in HEK293 cells, while prelamin A accumulation mimics inhibition of the degradation pathways (Fig. 3E). Consistent with the possibility that prelamin A anchors and stabilizes SUN1 at the nuclear envelope, we found that overexpression of the double-prelamin A mutant which is unable to bind SUN1 (LA L647R/R527P, Fig. 3C) (43), while triggering SUN1 mRNA expression (Fig. 3D), failed to increase SUN1 staining in nuclei (Fig. C and F). Thus, both increased mRNA levels and protein anchorage contribute to SUN1 recruitment to the nuclear envelope.

It has been recently shown SUN1 recruitment at the nuclear envelope of progeria fibroblasts accumulating prelamin A (43), suggesting that recruitment of SUN1 by prelamin A occurs in diverse cell types. This hypothesis was supported by data obtained in human myoblasts. While overexpression of prelamin A in cycling myoblasts did not significantly affect SUN1 or SUN2 staining in the majority of nuclei (Fig. 1, supplemental material), overexpression of prelamin A mutants in

resting myoblasts influenced SUN1 staining at the nuclear envelope (Fig. 3G). SUN2 fluorescence intensity was not significantly affected by prelamin A in transfected myoblasts (Fig. 3G). SUN1 labeling was increased in cells transfected with uncleavable prelamin A (LA-L647R), while a variable effect was obtained using LA-WT and LA-C661M (Fig. 3 G). We could not completely rule out that SUN1-containing complexes, more tightly associated with insoluble structures, may include non-farnesylated prelamin A, since, co-localization of non-farnesylated prelamin A and SUN1 was observed at the nuclear rim and in nuclear aggregates (Fig. 3 G). However, the whole evaluation of the above reported data allowed us to conclude that farnesylated prelamin A is the only form of the lamin A precursor recovered in normal differentiating human myoblasts and mature muscle and to suggest that prelamin A influences SUN1 anchorage at the nuclear envelope of differentiating human muscle cells.

Mislocalization of prelamin A and SUN2 in mevinolin-treated myotubes

To start addressing the relevance of prelamin A farnesylation and SUN1 modulation in human muscle, we wondered if changes in the post-translational modification harbored by prelamin A would have affected SUN1 expression and/or myoblast differentiation. Hence, we treated differentiating human myoblasts with mevinolin, an HMG-CoA reductase inhibitor known to impair farnesylation of prelamin A, thus eliciting accumulation of the non-farnesylated lamin A precursor.

In mevinolin-treated samples, we evaluated prelamin A localization, SUN1 and SUN2 staining and myonuclear distribution.

As expected, 1188-2 antibody stained untreated myotube cultures, but failed to label mevinolin-treated cells (Fig. 4A, panels a, b). Consistently, antibodies directed to full-length prelamin A brightly stained the nuclear envelope in mevinolin-treated cells,

while they did not stain untreated samples (Fig. 4A, panels c-f show antibody 1188-1 staining). Non-farnesylated prelamin A was not enriched at the nuclear poles, contrary to what observed for the farnesylated form, but it was evenly distributed along the nuclear rim in most of the examined nuclei (Fig.4A, d, f). A minor percentage of nuclei showed mislocalization of non-farnesylated prelamin A and formation of enlarged aggregates (Fig. 4A, panel f). The intensity of SUN2 fluorescence staining was not or slightly affected by mevinolin treatment (Fig. 4A, panels g-l). However, enrichment of SUN2 at the nuclear poles was completely lost in treated cells (Fig. 4A, panels h, l and statistics in B). These observations suggested that a specific localization of prelamin A and SUN2 in myotubes is maintained through an intermediate binding partner recruited by farnesylated prelamin A, while other prelamin A forms and/or mature lamin A anchor SUN2 all over the nuclear envelope.

SUN1 recruitment is reduced in mevinolin-treated myotubes

Treatment of cycling myoblasts with mevinolin did not affect SUN1 levels (Fig. 2, supplemental material). However, the increase in SUN1 staining observed in control myotubes, was not detectable in 60 to 70% of myotubes subjected to mevinolin treatment (Fig. 4A, panels n, p and statistics in C). This result demonstrated that accumulation of farnesylated prelamin A, but not its unprocessed form, causes upregulation and recruitment of SUN1 to the nuclear envelope, in human myotubes. Indeed, SUN1 protein levels were reduced in cells subjected to mevinolin treatment, as determined by Western blot analysis (Fig. 4C). Overexpression of FLAG-prelamin A in human myotubes, supported these results (Fig. 1, supplemental material). In cells overexpressing wild-type prelamin A or LA-L647R prelamin A, SUN1 levels were not substantially affected (Fig. 1, supplemental material). We interpreted these results by considering that accumulation of SUN1 in the nuclear envelope (that occurs

in untransfected myotubes) cannot be further enhanced by overexpression of farnesylated prelamin A. Conversely, in agreement with the effect observed in mevinolin-treated cells, overexpression of LA-C661M, which elicits accumulation of non-farnesylated prelamin A, lowered SUN1 levels in 30% of myotube nuclei (Fig. 1, supplemental material). Since accumulation of non-farnesylated prelamin A in cycling myoblasts did not influence SUN1 levels, while endogenous prelamin A was not detected at that stage, we suggest that SUN1 expression in cycling muscle cells may be regulated by other factors. Moreover, SUN2 protein levels, which were not affected by mevinolin treatment (Fig. 4C), appear to be independent of prelamin A.

Clustering of nuclei in myotubes accumulating non-farnesylated prelamin A

Myotubes treated with mevinolin showed mislocalization of nuclei into enlarged clusters at the extremities of multinucleated cells (Fig. 4A and statistics in B, $p<0.05$ in treated versus untreated myotubes). Further, we found unordered arrangement of myonuclei within each cluster, along with high variability of myonuclear size and morphology (Fig. 4A and statistics in B). These results indicated that farnesylated prelamin A is involved in myonuclear anchorage or incorporation within myotubes. Clustering of nuclei mostly occurred in myotubes showing well-organized sarcomeres and more than 12 nuclei (Fig. 4A, panels b, f, l, p), suggesting that farnesylated prelamin A could play a major role in the formation of secondary myotubes. Along this line, recent reports show that SUN1 and SUN2 play a critical role in nuclear positioning in mouse muscle (7). Moreover, altered organization of nuclei at the neuromuscular junctions, associated with SUN2 mislocalization, has been demonstrated in muscle from laminopathic mouse models (13). Regarding the role of prelamin A-and SUNs in nuclear positioning, we propose the following mechanism. Farnesylated prelamin A accumulation triggers upregulation of SUN1 and favors

localization of SUN2 at the nuclear poles. Both SUN1 and SUN2, known to interact with centrosomal constituents (11, 44, 45), drive nuclear movement through cytoskeleton binding. In this context, a role of the prelamin A and SUN1 binding partner emerin, implicated in centrosome positioning (46) and undergoing modulation and cytoskeleton binding during myogenesis (47, 48), appears likely. However, an interplay between SUNs, prelamin A and centrosomal proteins in human myoblasts deserves further investigation.

Physiological relevance of SUN1-prelamin A interplay

Persistence of SUN1 and prelamin A in mature muscle, hinted at the existence of a molecular complex involved not only in myogenesis, but also in muscle homeostasis. To evaluate the physiological relevance of SUN1-prelamin A interplay, we examined protein distribution in human myofibers at different ages. Prelamin A and SUN1 underwent parallel modulation, with myofibers from younger individuals (4 months) showing faint or absent labeling of both proteins at the nuclear rim (Fig. 5A). SUN1 and prelamin A staining increased in adult and aged muscle. Bright staining of both nuclear constituents was observed starting at age 20 up to age 82 in all muscle and connective tissue nuclei (Fig. 5A). The modulation of prelamin A and SUN1 levels here shown during muscle development and ageing (Fig. 5A-B) is consistent with the possibility that both proteins might regulate nucleo-cytoskeleton relationships in adult to aged muscle. Importantly, it has been shown that SUN proteins are dispensable for muscle development in the embryo, while they play a key role in muscle homeostasis (7). Moreover, it has been reported that myonuclear domains are differently organized in young, adult or aged muscle (1), suggesting age-related modulation of proteins, such as SUN1, regulating nuclear positioning and cytoskeleton interplay.

Low farnesylated prelamin A and SUN1 levels in EDMD myoblasts associated with clustering of myonuclei

LMNA mutations causing muscle laminopathies may interfere with prelamin A-SUN1 interaction (43). Moreover, altered myonuclear positioning and chromatin defects have been reported in laminopathic muscle (13, 49, 50). Based on these published data and on the new findings here obtained in normal human muscle, we wondered if *LMNA* pathogenetic mutations might affect SUN1 expression or recruitment to the nuclear envelope. In autosomal EDMD (EDMD2) myoblasts, we observed indeed lower levels of farnesylated prelamin A and SUN1 (Fig. 5C, D), while non-farnesylated prelamin A was not detected. About 40% of myotube nuclei were negative for prelamin A and SUN1 labeling ($p<0.05$ in 100 counted nuclei from 3 different EDMD cultures versus controls). Importantly, highly differentiated myotubes showed nuclear clustering and misshapening (Fig. 5C, D), reminiscent of what observed in wild-type myotubes in the absence of farnesylated prelamin A (Fig. 4). In mature muscle, both SUN1 and prelamin A levels were slightly affected by *LMNA* mutations (Fig. 5E). Nuclear clustering, however, was observed in longitudinal fibers (Fig. 5E, F). We suggest that reduced prelamin A and SUN1 recruitment in EDMD2 primarily affects satellite cells activity and myotube formation. However, downstream effects including clustering of myonuclei may progressively accumulate in mature muscle.

Conclusion

The functional connection between the cytoskeleton and the nucleus involves proteins of the so-called LINC complex (after linker of cytoskeleton and nucleoskeleton), including SUNs and nesprins (51). It is possible that SUN proteins not only regulate nuclear anchorage, but also co-ordinate positioning of chromatin domains with respect to that of the nucleus (52, 53). This intriguing function appears to be particularly relevant in differentiating myoblast nuclei, which undergo dramatic changes in their structure, location and higher order chromatin arrangement (1).

Here we show that SUN1 expression is modulated during differentiation of human muscle progenitors in a farnesylated prelamin A dependent way. Our data further hint at the existence of a molecular complex including SUN1 and prelamin A, which could be involved in adult muscle homeostasis. The interplay between prelamin A and SUN proteins is implicated in myonuclear positioning in healthy human muscle. Hence, myonuclear positioning is affected by the low levels of farnesylated prelamin A and SUN1 found in EDMD2 myoblasts. Thus, we suggest that prelamin A levels and post-translational modifications are crucial to protein functionality in myogenic progenitors.

The perspective of our study will be to identify modulators of prelamin A levels as well as other binding partners of farnesylated prelamin A and/or SUNs, relevant to the described effects in human muscle. For instance, FHL1, nesprin 1 and 2 represent good candidates, because they are involved in myonuclear positioning (44, 54) and myotube hypertrophy (3), and are indeed mutated in EDMD (55, 56).

Our results suggest that muscle atrophy or misfunctioning found in progeria (28) and mandibuloacral dysplasia (29) could be related to impaired modulation of prelamin A processing and downstream effects on SUN1 recruitment.

On the other hand, it has been recently reported that accumulation of non-farnesylated prelamin A causes cardiomyopathy in mice (57). This finding supports our observations in skeletal muscle and suggests that prelamin A-SUN1 interplay deserves investigation in cardiac myocytes. Finally, as hypothesised by diverse authors, it appears likely that mutations in SUN1 or SUN2 might be linked to laminopathies.

MATERIALS AND METHODS

Cell culture and transfection

Human myoblast cultures were obtained from muscle biopsies by mechanical and enzymatic methods, as previously reported (58). Biopsies were obtained from 10 consenting patients undergoing orthopedic surgery for traumas. Biopsies from 3 EDMD2 patients undergoing diagnosis were used to establish primary myoblast cultures or cryosectioned to analyze protein localization. All the local and EU ethical issues were respected. Mutations found in EDMD2 muscle were: *LMNA* R190Q/R249Q, *LMNA* Y259D, *LMNA* L140P (58).

To obtain myotubes, confluent cell cultures were allowed to differentiate in culture medium (D-MEM plus 20% FCS plus antibiotics) for 8 days. Cells cultured for 3-4 days post-confluence were defined as resting cells if 4-8 myotubes per dish (P100 dishes) were counted. PCNA staining of these cultures was negative in 70% of nuclei.

HEK293 cells were transfected with FLAG-tagged plasmids containing wild-type prelamin A, LA-WT, which undergoes normal maturation; LA-C661M, which cannot be farnesylated and LA-L647R, which is farnesylated but cannot undergo endoproteolysis (35) (Fig. 3A). The LA-R527P and LA-L647R/R527P prelamin A constructs (Fig. 3A), which carry the pathogenetic mutation R527P causing EDMD2 (43, 49) were also transfected in HEK293 cells. Transfections were performed using calcium phosphate buffer, whereas human myoblasts and myotubes were transfected using an AMAXA electroporator according to the manufacturer's instructions. After transfection, cells were incubated for 24-48 hours (22).

When indicated, the proteasome inhibitor MG132 (1 μM for 24 hours) or the lysosomal activity inhibitor chloroquine-diphosphate (25 μM for 18 hours) were added to transfected HEK293 cells to study SUN1 degradation.

Accumulation of non-farnesylated prelamin A was obtained using 10 μM mevinolin (Sigma) in growth medium for 48 hours (59).

Real-time PCR

Total RNA was extracted using the TRIzol extraction kit (Invitrogen). Real-time PCR was performed on the panel of HEK293 cells transfected with prelamin A constructs (LA-WT, LA-C661M, LA-L647R, LA-L647R/R527P or the empty vector) for 24 hours. In particular, 500 ng of total RNA was reverse-transcribed with high capacity cDNA archive kit (Applied Biosystems, Foster City, CA). Gene-specific primers were designed using Beacon Designer software : SUN1 (accession # NM_001130965.2), forward 5'-CAG AAG CAC AAA CAA ATC-3' and reverse 5'-CAC CAT CAT CAT CAA GAC-3'; glyceraldehyde-3-phosphate dehydrogenase (GAPDH) was amplified as endogenous control (forward 5'-GAA GGT GAA GGT CGG AGT C-3' and reverse 5'-GAA GAT GGT GAT GGG ATT TC-3' . Amplification was performed at the following cycling conditions: 95°C for 10 min followed by 40 cycles at 95°C for 15 s and 55°C for 1 min. A SYBR Green PCR Master Mix (Applied Biosystems) was used with 5 ng of cDNA and with 300 nM primers. No template controls were run with every assay performed on ABI PRISM 7900 Sequence Detection System (Applied Biosystems). Data were normalized to GAPDH and expressed as relative amount of SUN1 mRNA in transfected cell lines compared to the empty vector transfected calibrator. All data are expressed as $2^{-\Delta\Delta CT}$. Data were obtained from triplicate experiments.

Immunofluorescence and immunohistochemistry

Cells were grown on glass coverslips and immunofluorescence staining was performed in samples fixed in 100% methanol for 7 minutes. Unfixed cryosections were saturated 45 minutes with 4% BSA prior to immunofluorescence reactions (58). Three different antibodies were used to detect prelamin A: antibody 1188-1 (Diatheva), which is directed against the last 15 aminoacids of the full length protein; antibody 1188-2 (Diatheva), which selectively binds farnesylated prelamin A devoid of the last three aminoacids (Fig. 3, supplemental material) (37); Sc-6214 anti-prelamin A antibody (Santa Cruz), which is directed against the 20 C-terminal aminoacids of the full length lamin A precursor (60) (Fig. 1B) All prelamin A antibodies were used at 1:100 dilution, except 1188-2 antibody which was used at 1:10 dilution. Rabbit polyclonal anti-SUN2 and SUN1 antibodies (9, 10) were from Atlas and were used at 1:800 and 1:300 dilution, respectively. Goat polyclonal anti-SUN1 was from Santa Cruz. Anti-caveolin 3 antibody (BD-Transduction) was diluted 1:30, anti-desmin (Novocastra) was diluted 1:100, anti-dystrophin (Novocastra) was incubated at 1:10 dilution. Texas red-conjugated alpha-bungarotoxin (Molecular probes) was used to label neuromuscular junctions. Anti-β1D integrin (Chemicon) was used to recognize myotendinous junctions.

Immunofluorescence microscopy was performed using a Nikon E600 epifluorescence microscope and a Nikon oil-immersion objective [100× magnification, 1.3 NA (numerical aperture)]. Photographs were taken using a Nikon digital camera (DXm) and NIS-Element BR2.20 software (Nikon). All images were taken at similar exposures within an experiment for each antibody. Image quantification was performed using NIS-Element BR2.20 software.

Images were processed using Adobe Photoshop 7.0 software (Adobe Systems).

Nuclear fractioning

To obtain nuclear fractions, cells detached with trypsin were incubated in cold hypotonic buffer containing 10mM Tris-HCl and protease inhibitors. Mechanical separation was then performed with a syringe and centrifugation of nuclei was performed at 1100 rpm for 10 minutes. Nuclei were lysed in buffer containing 50mM TRIS-HCl, 1% SDS containing or not 5% 2-mercaptoethanol. Some samples were heated at 70°C to check the stability of SUN1 dimers, while other samples were obtained in the absence of 2-mercaptoethanol (10). Lysates were subjected to SDS-PAGE and Western blot analysis as described below.

Immunoprecipitation and immunoblotting

Immunoprecipitation was performed in transfected HEK293 cells overexpressing prelamin A mutants, according to a procedure reported in previous studies (36). Briefly, HEK293 cells were lysed in IP buffer containing 50 mM HEPES/HCl (pH 7.4), 100 mM NaCl, 1.5 mM MgCl2, 1% NP-40, 1 mM dithiothreitol, 1 mM PMSF and protease inhibitors. After sonication and clarification, 500 µg of each lysate were incubated with anti-FLAG antibody overnight at 4◦C. Control immunoprecipitations were performed in the presence of non-specific immunoglobulins. After addition of 30 µl of Protein A/G (Santa Cruz Biotechnology), lysates were incubated with continuous mixing at 4◦C for 3 h. Immunoprecipitated protein complexes were subjected to Western-blot analysis.

Western blot analysis was performed on proteins separated by a 5-20% gradient SDS-PAGE. Nitrocellulose membranes were probed using the following antibodies : anti-FLAG (Sigma, 1:1000 dilution); rabbit polyclonal anti-SUN2 and SUN1 (Atlas, 1:200 and 1:100 dilution respectively); anti-prelamin A (1188-1, Diatheva, 1:100 dilution); anti-emerin (Monosan, 1:100 dilution); anti-myogenin (Santa Cruz, 1:100 dilution). Immunoblotted bands were revealed by the Amersham ECL® detection system. The

intensity of bands was measured using a GS800 Densitometer (Biorad).

Statistical analysis

Statistical analysis was performed using Excel software (Microsoft). Statistically significant differences were determined using the Student's t test.

ACKNOWLEDGEMENTS

The authors wish to thank William Blalock (Cell Signaling Laboratory, Department of Human Anatomical Sciences, University of Bologna) for revising the manuscript and for the helpful discussion, Clara Guerzoni for the evaluation of the expression study, P. Sabatelli, A. Valmori, O. Fiorani, S. Grasso and D. Zini for the technical assistance. This work was supported by grants from: A.I.Pro.Sa.B., Italy; EU-funded FP6 Euro-Laminopathies project; Italian MIUR PRIN 2008 to G.L.; ISS 'Rare Diseases Italy–U.S.A. program [grant number 526/D30]; Telethon grant # GUP08006 to L.M.; Fondazione Carisbo, Italy.

CONFLICTS OF INTEREST

None

REFERENCES

1. Wagers AJ, Conboy IM. Cellular and molecular signatures of muscle regeneration: current concepts and controversies in adult myogenesis. *Cell* 2005 Sep 9; **122** (5)**:** 659-667.

2. Horsley V, Friday BB, Matteson S, Kegley KM, Gephart J, Pavlath GK. Regulation of the growth of multinucleated muscle cells by an NFATC2-dependent pathway. *J Cell Biol* 2001 Apr 16; **153** (2)**:** 329-338.

3. Cowling BS, McGrath MJ, Nguyen MA, Cottle DL, Kee AJ, Brown S*, et al.* Identification of FHL1 as a regulator of skeletal muscle mass: implications for human myopathy. *J Cell Biol* 2008 Dec 15; **183** (6)**:** 1033-1048.

4. Milner DJ, Weitzer G, Tran D, Bradley A, Capetanaki Y. Disruption of muscle architecture and myocardial degeneration in mice lacking desmin. *J Cell Biol* 1996 Sep; **134** (5)**:** 1255-1270.

5. Srsen V, Fant X, Heald R, Rabouille C, Merdes A. Centrosome proteins form an insoluble perinuclear matrix during muscle cell differentiation. *BMC Cell Biol* 2009; **10:** 28.

6. Zhang X, Xu R, Zhu B, Yang X, Ding X, Duan S*, et al.* Syne-1 and Syne-2 play crucial roles in myonuclear anchorage and motor neuron innervation. *Development* 2007 Mar; **134** (5)**:** 901-908.

7. Lei K, Zhang X, Ding X, Guo X, Chen M, Zhu B*, et al.* SUN1 and SUN2 play critical but partially redundant roles in anchoring nuclei in skeletal muscle cells in mice. *Proc Natl Acad Sci U S A* 2009 Jun 23; **106** (25)**:** 10207-10212.

8. Fridkin A, Penkner A, Jantsch V, Gruenbaum Y. SUN-domain and KASH-domain proteins during development, meiosis and disease. *Cell Mol Life Sci* 2009 May; **66** (9)**:** 1518-1533.

9. Padmakumar VC, Libotte T, Lu W, Zaim H, Abraham S, Noegel AA*, et al.* The inner nuclear membrane protein Sun1 mediates the anchorage of Nesprin-2 to the nuclear envelope. *J Cell Sci* 2005 Aug 1; **118** (Pt 15)**:** 3419-3430.

10. Lu W, Gotzmann J, Sironi L, Jaeger VM, Schneider M, Luke Y*, et al.* Sun1 forms immobile macromolecular assemblies at the nuclear envelope. *Biochim Biophys Acta* 2008 Dec; **1783** (12)**:** 2415-2426.

11. Schulz I, Baumann O, Samereier M, Zoglmeier C, Graf R. Dictyostelium Sun1 is a dynamic membrane protein of both nuclear membranes and required for centrosomal association with clustered centromeres. *Eur J Cell Biol* 2009 Nov; **88** (11)**:** 621-638.

12. Wang Q, Du X, Cai Z, Greene MI. Characterization of the structures involved in localization of the SUN proteins to the nuclear envelope and the centrosome. *DNA Cell Biol* 2006 Oct; **25** (10)**:** 554-562.

13. Mejat A, Decostre V, Li J, Renou L, Kesari A, Hantai D*, et al.* Lamin A/C-mediated neuromuscular junction defects in Emery-Dreifuss muscular dystrophy. *J Cell Biol* 2009 Jan 12; **184** (1)**:** 31-44.

14. Mittelbronn M, Sullivan T, Stewart CL, Bornemann A. Myonuclear degeneration in LMNA null mice. *Brain Pathol* 2008 Jul; **18** (3)**:** 338-343.

15. Prokocimer M, Davidovich M, Nissim-Rafinia M, Wiesel-Motiuk N, Bar D, Barkan R*, et al.* Nuclear lamins: key regulators of nuclear structure and activities. *J Cell Mol Med* 2009 Feb 4.

16. Marmiroli S, Bertacchini J, Beretti F, Cenni V, Guida M, De Pol A*, et al.* A-type lamins and signaling: the PI 3-kinase/Akt pathway moves forward. *J Cell Physiol* 2009 Sep; **220** (3)**:** 553-561.

17. Maraldi NM, Lattanzi G. Involvement of prelamin A in laminopathies. *Crit Rev Eukaryot Gene Expr* 2007; **17** (4)**:** 317-334.

18. Hakelien AM, Delbarre E, Gaustad KG, Buendia B, Collas P. Expression of the myodystrophic R453W mutation of lamin A in C2C12 myoblasts causes promoter-specific and global epigenetic defects. *Exp Cell Res* 2008 May 1; **314** (8)**:** 1869-1880.

19. Gotic I, Schmidt WM, Biadasiewicz K, Leschnik M, Spilka R, Braun J*, et al.* Loss of LAP2alpha Delays Satellite Cell Differentiation and Affects Postnatal Fiber Type Determination. *Stem Cells* 2009 Dec 28.

20. Muchir A, Wu W, Worman HJ. Reduced expression of A-type lamins and emerin activates extracellular signal-regulated kinase in cultured cells. *Biochim Biophys Acta* 2009 Jan; **1792** (1)**:** 75-81.

21. Cenni V, Bertacchini J, Beretti F, Lattanzi G, Bavelloni A, Riccio M*, et al.* Lamin A Ser404 is a nuclear target of Akt phosphorylation in C2C12 cells. *J Proteome Res* 2008 Nov; **7** (11)**:** 4727-4735.

22. Capanni C, Del Coco R, Squarzoni S, Columbaro M, Mattioli E, Camozzi D*, et al.* Prelamin A is involved in early steps of muscle differentiation. *Exp Cell Res* 2008 Dec 10; **314** (20)**:** 3628-3637.

23. Frock RL, Kudlow BA, Evans AM, Jameson SA, Hauschka SD, Kennedy BK. Lamin A/C and emerin are critical for skeletal muscle satellite cell differentiation. *Genes Dev* 2006 Feb 15; **20** (4)**:** 486-500.

24. Favreau C, Delbarre E, Courvalin JC, Buendia B. Differentiation of C2C12 myoblasts expressing lamin A mutated at a site responsible for Emery-Dreifuss muscular dystrophy is improved by inhibition of the MEK-ERK pathway and stimulation of the PI3-kinase pathway. *Exp Cell Res* 2008 Apr 1; **314** (6)**:** 1392-1405.

25. Bonne G, Di Barletta MR, Varnous S, Becane HM, Hammouda EH, Merlini L*, et al.* Mutations in the gene encoding lamin A/C cause autosomal dominant Emery-Dreifuss muscular dystrophy. *Nat Genet* 1999 Mar; **21** (3)**:** 285-288.

26. Muchir A, Bonne G, van der Kooi AJ, van Meegen M, Baas F, Bolhuis PA*, et al.* Identification of mutations in the gene encoding lamins A/C in autosomal dominant limb girdle muscular dystrophy with atrioventricular conduction disturbances (LGMD1B). *Hum Mol Genet* 2000 May 22; **9** (9)**:** 1453-1459.

27. Fatkin D, MacRae C, Sasaki T, Wolff MR, Porcu M, Frenneaux M*, et al.* Missense mutations in the rod domain of the lamin A/C gene as causes of dilated cardiomyopathy and conduction-system disease. *N Engl J Med* 1999 Dec 2; **341** (23)**:** 1715-1724.

28. Hennekam RC. Hutchinson-Gilford progeria syndrome: review of the phenotype. *Am J Med Genet A* 2006 Dec 1; **140** (23)**:** 2603-2624.

29. Lombardi F, Gullotta F, Columbaro M, Filareto A, D'Adamo M, Vielle A*, et al.* Compound heterozygosity for mutations in LMNA in a patient with a myopathic and lipodystrophic mandibuloacral dysplasia type A phenotype. *J Clin Endocrinol Metab* 2007 Nov; **92** (11)**:** 4467-4471.

30. Garg A, Subramanyam L, Agarwal AK, Simha V, Levine B, D'Apice MR*, et al.* Atypical progeroid syndrome due to heterozygous missense LMNA mutations. *J Clin Endocrinol Metab* 2009 Dec; **94** (12)**:** 4971-4983.

31. Kirschner J, Brune T, Wehnert M, Denecke J, Wasner C, Feuer A*, et al.* p.S143F mutation in lamin A/C: a new phenotype combining myopathy and progeria. *Ann Neurol* 2005 Jan; **57** (1)**:** 148-151.

32. Corrigan DP, Kuszczak D, Rusinol AE, Thewke DP, Hrycyna CA, Michaelis S*, et al.* Prelamin A endoproteolytic processing in vitro by recombinant Zmpste24. *Biochem J* 2005 Apr 1; **387** (Pt 1)**:** 129-138.

33. Yang SH, Chang SY, Andres DA, Spielmann HP, Young SG, Fong LG. Assessing the efficacy of protein farnesyltransferase inhibitors in mouse models of progeria. *J Lipid Res* 2010 Feb; **51** (2)**:** 400-405.

34. Capanni C, Mattioli E, Columbaro M, Lucarelli E, Parnaik VK, Novelli G*, et al.* Altered pre-lamin A processing is a common mechanism leading to lipodystrophy. *Hum Mol Genet* 2005 Jun 1; **14** (11)**:** 1489-1502.

35. Lattanzi G, Columbaro M, Mattioli E, Cenni V, Camozzi D, Wehnert M*, et al.* Pre-Lamin A processing is linked to heterochromatin organization. *J Cell Biochem* 2007 Dec 1; **102** (5)**:** 1149-1159.

36. Capanni C, Del Coco R, Mattioli E, Camozzi D, Columbaro M, Schena E*, et al.* Emerin-prelamin A interplay in human fibroblasts. *Biol Cell* 2009 Sep; **101** (9)**:** 541-554.

37. Dominici S, Fiori V, Magnani M, Schena E, Capanni C, Camozzi D*, et al.* Different prelamin A forms accumulate in human fibroblasts: a study in

experimental models and progeria. *Eur J Histochem* 2009 Jan-Mar; **53** (1)**:** 43-52.

38. Randles KN, Lam le T, Sewry CA, Puckelwartz M, Furling D, Wehnert M*, et al.* Nesprins, but not sun proteins, switch isoforms at the nuclear envelope during muscle development. *Dev Dyn* 2010 Mar; **239** (3)**:** 998-1009.

39. Martini FJ, Valdeolmillos M. Actomyosin contraction at the cell rear drives nuclear translocation in migrating cortical interneurons. *J Neurosci* 2010 Jun 23; **30** (25)**:** 8660-8670.

40. Burke B, Roux KJ. Nuclei take a position: managing nuclear location. *Dev Cell* 2009 Nov; **17** (5)**:** 587-597.

41. Crisp M, Liu Q, Roux K, Rattner JB, Shanahan C, Burke B*, et al.* Coupling of the nucleus and cytoplasm: role of the LINC complex. *J Cell Biol* 2006 Jan 2; **172** (1)**:** 41-53.

42. Liu Q, Pante N, Misteli T, Elsagga M, Crisp M, Hodzic D*, et al.* Functional association of Sun1 with nuclear pore complexes. *J Cell Biol* 2007 Aug 27; **178** (5)**:** 785-798.

43. Haque F, Mazzeo D, Patel JT, Smallwood DT, Ellis JA, Shanahan CM*, et al.* Mammalian SUN protein interaction networks at the inner nuclear membrane and their role in laminopathy disease processes. *J Biol Chem* 2010 Jan 29; **285** (5)**:** 3487-3498.

44. Zhang X, Lei K, Yuan X, Wu X, Zhuang Y, Xu T*, et al.* SUN1/2 and Syne/Nesprin-1/2 complexes connect centrosome to the nucleus during neurogenesis and neuronal migration in mice. *Neuron* 2009 Oct 29; **64** (2)**:** 173-187.

45. Xiong H, Rivero F, Euteneuer U, Mondal S, Mana-Capelli S, Larochelle D*, et al.* Dictyostelium Sun-1 connects the centrosome to chromatin and ensures genome stability. *Traffic* 2008 May; **9** (5)**:** 708-724.

46. Salpingidou G, Smertenko A, Hausmanowa-Petrucewicz I, Hussey PJ, Hutchison CJ. A novel role for the nuclear membrane protein emerin in association of the centrosome to the outer nuclear membrane. *J Cell Biol* 2007 Sep 10; **178** (6)**:** 897-904.

47. Lattanzi G, Ognibene A, Sabatelli P, Capanni C, Toniolo D, Columbaro M*, et al.* Emerin expression at the early stages of myogenic differentiation. *Differentiation* 2000 Dec; **66** (4-5)**:** 208-217.

48. Lattanzi G, Cenni V, Marmiroli S, Capanni C, Mattioli E, Merlini L*, et al.* Association of emerin with nuclear and cytoplasmic actin is regulated in differentiating myoblasts. *Biochem Biophys Res Commun* 2003 Apr 11; **303** (3)**:** 764-770.

49. Sabatelli P, Lattanzi G, Ognibene A, Columbaro M, Capanni C, Merlini L*, et al.* Nuclear alterations in autosomal-dominant Emery-Dreifuss muscular dystrophy. *Muscle Nerve* 2001 Jun; **24** (6)**:** 826-829.

50. Hale CM, Shrestha AL, Khatau SB, Stewart-Hutchinson PJ, Hernandez L, Stewart CL*, et al.* Dysfunctional connections between the nucleus and the actin and microtubule networks in laminopathic models. *Biophys J* 2008 Dec; **95** (11)**:** 5462-5475.

51. Ostlund C, Folker ES, Choi JC, Gomes ER, Gundersen GG, Worman HJ. Dynamics and molecular interactions of linker of nucleoskeleton and cytoskeleton (LINC) complex proteins. *J Cell Sci* 2009 Nov 15; **122** (Pt 22)**:** 4099-4108.

52. Penkner AM, Fridkin A, Gloggnitzer J, Baudrimont A, Machacek T, Woglar A*, et al.* Meiotic chromosome homology search involves modifications of the nuclear envelope protein Matefin/SUN-1. *Cell* 2009 Nov 25; **139** (5)**:** 920-933.

53. Ding X, Xu R, Yu J, Xu T, Zhuang Y, Han M. SUN1 is required for telomere attachment to nuclear envelope and gametogenesis in mice. *Dev Cell* 2007 Jun; **12** (6)**:** 863-872.

54. Zhang J, Felder A, Liu Y, Guo LT, Lange S, Dalton ND*, et al.* Nesprin 1 is critical for nuclear positioning and anchorage. *Hum Mol Genet* 2010; **19** (2)**:** 329-341.

55. Gueneau L, Bertrand AT, Jais JP, Salih MA, Stojkovic T, Wehnert M*, et al.* Mutations of the FHL1 gene cause Emery-Dreifuss muscular dystrophy. *Am J Hum Genet* 2009 Sep; **85** (3)**:** 338-353.

56. Zhang Q, Bethmann C, Worth NF, Davies JD, Wasner C, Feuer A*, et al.* Nesprin-1 and -2 are involved in the pathogenesis of Emery Dreifuss muscular dystrophy and are critical for nuclear envelope integrity. *Hum Mol Genet* 2007 Dec 1; **16** (23)**:** 2816-2833.

57. Davies BS, Barnes RH, 2nd, Tu Y, Ren S, Andres DA, Spielmann HP*, et al.* An accumulation of non-farnesylated prelamin A causes cardiomyopathy but not progeria. *Hum Mol Genet* 2010 May 4.

58. Cenni V, Sabatelli P, Mattioli E, Marmiroli S, Capanni C, Ognibene A*, et al.* Lamin A N-terminal phosphorylation is associated with myoblast activation: impairment in Emery-Dreifuss muscular dystrophy. *J Med Genet* 2005 Mar; **42** (3)**:** 214-220.

59. Mattioli E, Columbaro M, Capanni C, Santi S, Maraldi NM, D'Apice MR*, et al.* Drugs affecting prelamin A processing: effects on heterochromatin organization. *Exp Cell Res* 2008 Feb 1; **314** (3)**:** 453-462.

60. Gruber J, Lampe T, Osborn M, Weber K. RNAi of FACE1 protease results in growth inhibition of human cells expressing lamin A: implications for

Hutchinson-Gilford progeria syndrome. *J Cell Sci* 2005 Feb 15; **118** (Pt 4)**:** 689-696.

TITLES AND LEGENDS TO FIGURES

Figure 1. SUN1, SUN2 and farnesylated prelamin A modulation in human muscle progenitors. (A) Cycling myoblasts (cycling), committed myoblasts (day 3, caveolin positive mononucleated cells) and myotubes (day 8, caveolin positive multinucleated cells) are shown. Cells negative for caveolin 3 staining in panels b-e, h-m and p-s are resting myoblasts (indicated by arrowheads). Nuclei were stained with antibodies directed to SUN1 (a-e), SUN2 (g-m) or farnesylated prelamin A (o-s). Caveolin 3 was detected using TRITC-conjugated anti-mouse IgG (red), SUN1, SUN2 and prelamin A were detected using FITC-conjugated secondary antibodies (green). Nuclei shown in day 8 myoblasts were counterstained with DAPI (f, n, t). (B) Prelamin A forms detected by the three antibodies used in this study. Epitopes detected by anti-prelamin A antibodies are colored in light blue. Anti-prelamin A 1188-1 antibody detects full- length prelamin A (aminoacids 648-664, prelamin A-specific), Sc-6214 antibody binds full-length prelamin A (aminoacids 645-664), 1188-2 antibody detects farnesylated prelamin A (aminoacids 648-661 including farnesyl-cysteine 661 and devoid of the SIM sequence), but not full-length prelamin A (37). The farnesyl group is depicted as "F" within a green circle. The prelamin A –specific sequence starts at aminoacid 648 (yellow bar). (C) Cycling myoblasts (a-c), day 3 myoblasts (d-f) and day 8 myoblasts (g-i) were labeled using three different anti-prelamin A antibodies (green). The code of each antibody is reported on the left. Cytoplasms were stained with anti-desmin antibody, as a muscle-specific marker (red staining). (D) The percentage of nuclei showing prelamin A staining, detected by antibodies 1188-1, Sc-6214 or 1188-2 is reported in the graph as means ± standard deviation of three different counts (100 nuclei per count). Examined samples are: cycling myoblasts (cycling), resting myoblasts (resting), myotubes and committed

cells (myotubes). Asterisks indicate statistically significant differences at the Student's t-test ($p<0.05$), with respect to resting myoblast values. Samples were obtained from 3 different donors. (E) Western blot analysis of SUN1, SUN2, lamin A/C and myogenin was performed in nuclear lysates from cycling myoblasts (cycling), day 3 myoblasts (day 3) or day 8 myoblasts (day 8). Myogenin was used as a differentiation marker. Ponceau staining of a representative band shows equal protein loading. Western blot analysis showing different stability of the SUN1 200 kDa band (asterisk) under reducing or non-reducing conditions is shown in the lower panel. 2-Me, 2-mercaptoethanol; 70°, samples heated at 70°C in the presence of 2-mercaptoethanol. Equal number of nuclei was loaded per each sample. Myogenin is used as a differentiation marker also showing equal protein loading. Molecular weight markers are reported in kDa. Experiments were repeated three times under the same conditions. (F) Densitometric analysis of SUN1 (100 kDa) and SUN2 immunoblotted bands was performed in triplicate experiments and the mean values ± standard deviation are reported. Statistically significant differences ($p<0.05$), with respect to values determined in day 3 myoblasts are indicated by asterisks in the bars. Cycling, cycling myoblasts; day3, day 3 post-confluence; day8, day 8 post-confluence. Bars in (A) and (C), 10 µm.

Figure 2. Localization of SUN1, SUN2 and prelamin A in human muscle cells. (A) Colocalization of farnesylated prelamin A (prelamin A, green) and SUN1 (SUN1, red) in human myotubes (day 8 post-confluence). Prelamin A staining is not observed in resting cells (arrowheads), while SUN1 levels are reduced. Bar, 10 µm. (B) Mean fluorescence intensity of SUN2, SUN1 and prelamin A in nuclei of cycling myoblasts (cycling), resting myoblasts (resting) and myotubes (myotubes) measured by the NIS software analysis system. 300 nuclei per sample were counted. (C) Emerin (panels a-

b), SUN2 (panels d-e), farnesylated prelamin A (panels g-h) and SUN1 (panels l-m) were labeled using specific antibodies and detected using FITC-conjugated secondary antibodies (green). Caveolin 3 (red) was used as a differentiation marker (panels b, e, h, m). Counterstaining of DNA with DAPI is shown in panels c, f, i, n. Arrows indicate protein enrichment at the nuclear poles. (D) Differentiated myoblasts transfected with FLAG-tagged LA-L647R prelamin A were labeled using anti-FLAG (red) and anti-SUN2 (green) antibodies. Colocalization of proteins (arrows) and DAPI counterstaining are shown in the merged image (merge). (E) The percentage of nuclei with enrichment of staining at the nuclear pole(s) is reported in the graph as mean values ± standard deviation of three different counts. One hundred of nuclei per each experiment were counted. Examined samples were committed myoblasts or myotubes, as reported below the bars. (F) Higher magnification of nuclear poles labeled by anti-emerin, SUN2, prelamin A or SUN1 antibodies shows polarization of proteins. (G) Fluorescence intensity profile of the nuclear rim from cells co-stained using anti-emerin and anti-SUN2, prelamin A or SUN1 antibodies. Analysis was performed using NIS elements 2.2, on 50 labeled nuclei per sample. Emerin profile was uniform (upper left panel and black profile in the other panels) and it was used as a control of nuclear shape.

(H) SUN2, prelamin A and SUN1 staining in cryosections from human paravertebral muscles (100 nuclei in each sample from 3 different biopsies). Non-synaptic muscle fibers (NMF) are shown in a, b and c. Myotendinous junctions (MTJ) are shown in d-f (sarcolemma was labeled using anti-beta 1D integrin antibody). Neuromuscular junctions (NMJ) are shown in g-i: acetylcoline receptors were stained using Texas red-conjugated alpha-bungarotoxin (red). Corresponding nuclei in serial cryosections are indicated by arrows. All the bars, 10 μm.

Figure 3. Potential mechanisms of SUN1 regulation by prelamin A. (A) Prelamin A sequences expressed in this study. Cells were transfected with cDNAs encoding for LA-WT (processable prelamin A), LA-C661M (non-farnesylable prelamin A) or LA-L647R (uncleavable farnesylated prelamin A) LA-L647R/R527 prelamin A double mutant and LA-R527H processable prelamin A. Protein domains are reported in figure row. Mutations are reported in green. (B) SUN1 and SUN2 expression in HEK 293 cells transfected with prelamin A forms. The percentage of transfected cells ranged 80-90%. SUN1 and SUN2 were labeled using specific antibodies and revealed by FITC-conjugated secondary antibody (green). Overexpressed proteins were detected using a Cy3-conjugated anti-FLAG antibody (red). (C) Left panel: western blot analysis of SUN1 and SUN2 in transfected HEK293 cells was performed using nuclear lysates (nuclear lysates). Mock, mock-transfected cells. Co-immunoprecipitation of FLAG-tagged prelamin A and SUNs was performed using an anti-FLAG antibody (FLAG-IP) in nuclear lysates. Proteins were detected using anti-SUN1, SUN2, FLAG or emerin antibody. SUN1 co-immunoprecipitated with LA-L647R prelamin A only. A/G, control precipitations performed with antibody free buffer. Right panel: densitometric analysis of SUN1 and SUN2 immunoblotted bands obtained from HEK293 nuclear lysates analyzed in triplicate western blots. Mean values ± standard deviation are reported. Statistically significant differences with respect to mock transfected cells values were determined by Student's t test ($p<0.05$). (D) Real-time RT-PCR of SUN1 transcripts in HEK293 cells mock-transfected (mock) or transfected with LA-WT, LA-C661M, LA-L647R or LA-L647R/R527P for 24 hours. LA-C661M elicits SUN1 downregulation, while LA-L647R causes a 3-fold upregulation of SUN1. (E) Accumulation of SUN1 at the nuclear envelope in HEK293 cells treated with the lysosome inhibitor chloroquine (CQ) or the proteasome inhibitor MG132 (MG132). SUN1 was stained with specific antibody and revealed by

FITC-conjugated secondary antibody (green). Nuclei were counterstained with DAPI. (F) Overexpression of mutant prelamin A which cannot bind SUN1 (LA-R527P or LA-L647R/R527P) fails to elicit recruitment of SUN1 to the nuclear envelope. LA-L647R farnesylated prelamin A was overexpressed as a positive control. Overexpressed proteins were revealed by Cy3-conjugated anti-FLAG antibody (red), SUN1 was labeled with specific antibody (green). (G) Human myoblasts (resting cells, day 3 post-confluence) were transfected with LA-WT, LA-C661M or LA-L647R cDNAs and fixed 48 hours after transfection. SUN1 and SUN2 were labeled using specific antibodies and revealed by FITC-conjugated secondary antibody (green). Overexpressed proteins were detected using Cy3-conjugated anti-FLAG antibody (red). Bars in (B), (E), (F) and (G), 10 µm.

Figure 4. Reduced levels of farnesylated prelamin A affect SUN1 expression and nuclear positioning in myotubes. (A) Differentiating myoblasts (day 6 post-confluence) were left untreated (untreated) or treated with mevinolin for 48 hours (mevinolin). Cell cultures were fixed at day 8 post-confluence. Highly differentiated myotubes (more than 12 nuclei) are shown in panels a, b, e, f, i, l, o, p. Myotubes with less than 6 nuclei are shown in panels c, d, g, h, m, n. Farnesylated prelamin A was detected using 1188-2 antibody (a, b, red). Full-length prelamin A (non-farnesylated prelamin A) was detected using 1188-1 antibody (c-f, red). SUN2 was detected using anti-SUN2 antibody (g-l, red). SUN1 was detected using anti-SUN1 antibody (m-p, red). Caveolin 3 (green) was stained as a marker of myogenic differentiation. Bar, 10 µm. Clustering of myotube nuclei (more than three agglomerated nuclei in unordered distribution on one side of the myotube, with myotube areas devoid of nuclei) is observed in mevinolin-treated cells (right lane). Misshapen nuclei (nuclei with blebs, invaginations or enlarged nuclei) are also observed (panels d, f, h).

(B) Statistical analysis (mean values ± standard deviation of counts performed in three different samples). Counting was performed in 100 myotube nuclei per each sample. Misshapen nuclei (misshapen) or nuclei belonging to a cluster (clustered) were counted in myotubes left untreated or treated with mevinolin (upper panel). Nuclei showing nuclear pole enrichment of SUN2 (detected using anti-SUN2 antibody) or prelamin A (detected using anti-prelamin A 1188-2 antibody in untreated cells and anti-prelamin A 1188-1 antibody in mevinolin-treated cells) were counted (middle panel). SUN1 or farnesylated prelamin A fluorescence intensity, labeled using anti-SUN1 or anti-prelamin A 1188-2 antibody respectively, was determined using the NIS software and registered for 100 nuclei (lower panel). All the differences between untreated and mevinolin-treated samples were statistically significant ($p < 0.05$). (C) Western blotting analysis of SUN1, SUN2, prelamin A and lamin A/C in untreated or mevinolin-treated (+mev) myotube cultures. Prelamin A was detected using anti-prelamin A 1188-1 antibody directed to the full-length protein. Emerin is used as a loading control. Molecular weight markers are reported in kDa. Densitometric values are reported as percentage of values registered in untreated samples and represent means ± standard deviation of three different experiments.

Figure 5. Physiological role of prelamin A/SUN1 interplay.

(A) SUN1 and farnesylated prelamin A staining in muscle cryosections from tibialis anterior of individuals at different age (control muscle). FITC-conjugated secondary antibodies were used to detect SUN1 and prelamin A (green). Nuclei were counterstained with DAPI. A representative nucleus at two-fold magnification is shown in the inset for each picture. m, months; y, years. (B) The percentage of farnesylated prelamin A (prelamin A) or SUN1 (SUN1) positive nuclei is reported as mean value of three different countings performed in two different samples of the

same age. m, months; y, years. (C) Myotubes from control (a,b) or EDMD2 (c,d) primary cultures were stained for farnesylated prelamin A (prelamin A) or SUN1 (SUN1) at day 8 post-confluence. Reduced protein levels and myonuclear clustering are observed in EDMD2 myotubes. Prelamin A and SUN1 were stained using specific antibodies and revealed by TRITC-conjugated secondary antibody (red). Caveolin 3 (green) was stained as a marker of myogenic differentiation. (D) Statistical analysis (mean values ± standard deviation of three different countings) performed in control and EDMD2 myotubes. Mutations are reported below the bars. SUN1 (SUN1) or farnesylated prelamin A (prelamin A) fluorescence intensity, labeled using anti-SUN1 or anti-prelamin A 1188-2 antibody respectively, was determined using the NIS software and registered for 100 nuclei (upper panel). Misshapen nuclei (misshapen) or nuclei belonging to a cluster (clustered) were counted and registered for 100 nuclei (lower panel). (E) Tibialis anterior muscle longitudinal sections from control (a,b and insets below each panel) or EDMD2 patients (c, d and insets below each panel) were stained for SUN1 (SUN1, a,c) or farnesylated prelamin A (prelamin A, b,d). Proteins were revealed by FITC-conjugated secondary antibody (green). Nuclei indicated by arrowheads are shown at 3-fold magnification in the insets. (F) Statistical analysis (mean values ± standard deviation of three different countings) performed in control and EDMD2 myofibers. Misshapen nuclei (misshapen) or nuclei belonging to a cluster (clustered) were counted and registered. 50 nuclei per sample were counted in longitudinal sections. Nuclei in (A), (C) and (E) were counterstained with DAPI. Bars in (A), (C) and (E) , 10 µm.

Figure 1s. Overexpression of prelamin A in human myoblasts affects SUN1 levels and localization. Cycling myoblasts (cycling), resting myoblasts (day 3 post-confluence, d3) or differentiated myoblasts (day 8 post-confluence, d8) were transfected with LA-WT, LA-C661M or LA-L647R and fixed 48 hours after transfection. FLAG staining (using a Cy3-conjugated primary antibody, red) was performed to detect overexpressed proteins. SUN1 was labeled using anti-SUN1 antibody and revealed by FITC-conjugated secondary antibody (green). Overexpression of unprocessable non-farnesylated prelamin A caused recruitment of SUN1 in intranuclear aggregates. In myotubes (d8), overexpression of LA-C661M elicited decrease of SUN1 fluorescence. Bar, 10 µm.

Figure 2s. Modulation of SUN1 in untreated and mevinolin-treated human myoblasts. Cycling myoblasts (cycling), resting myoblasts (day 3 post-confluence, d3) or differentiated myoblasts (day 8 post-confluence, d8) were left untreated or treated with 10 µM mevinolin for 48 hours. SUN1 was labeled using anti-SUN1 antibody and revealed by TRITC-conjugated secondary antibody (red). Mevinolin treatment did not affect SUN1 staining in mononucleated cells (cycling and d3), but caused decrease of SUN1 labeling and clustering of nuclei in myotubes. Misshapen nuclei are also observed in mevinolin-treated cells (compare nuclei indicated by arrowheads in d8 myotubes). Bar, 10 µm.

Figure 3s. Anti-prelamin A 1188-2 antibody saturation abolishes nuclear staining in human myotubes. Peptide saturation was performed for 1 hour at room

temperature using increasing concentrations of farnesyl-peptide (lamin A aminoacids 649-661 including farnesyl-cysteine 661).

The farnesyl-peptide was employed at 1.5 and 10 times the concentration of the antibodies used. Picture is representative of 10 times concentration. Bar, 10 μm.

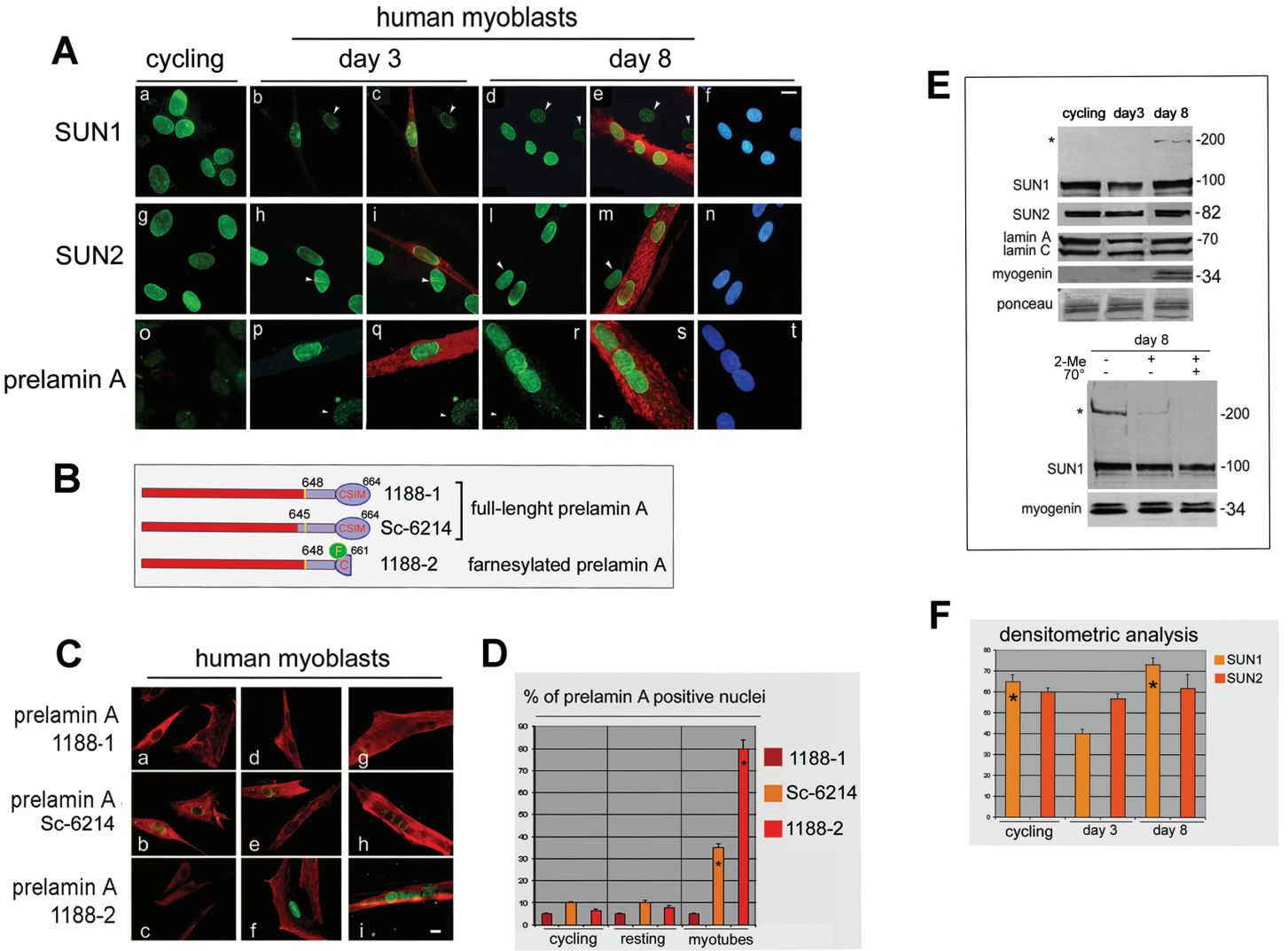
A
human myoblasts
cycling
day 3
day 8
SUN1
SUN2
prelamin A
B
648
664
CSIM
1188-1
full-lenght prelamin A
645
664
CSIM
Sc-6214
648
F
661
C
1188-2
farnesylated prelamin A
C
human myoblasts
prelamin A 1188-1
prelamin A Sc-6214
prelamin A 1188-2
D
% of prelamin A positive nuclei
1188-1
Sc-6214
1188-2
cycling
resting
myotubes
E
cycling day3 day 8
SUN1
SUN2
lamin A
lamin C
myogenin
ponceau
-200
-100
-82
-70
-34
day 8
2-Me
70°
SUN1
myogenin
-200
-100
-34
F
densitometric analysis
SUN1
SUN2
cycling
day 3
day 8

Figure 1.

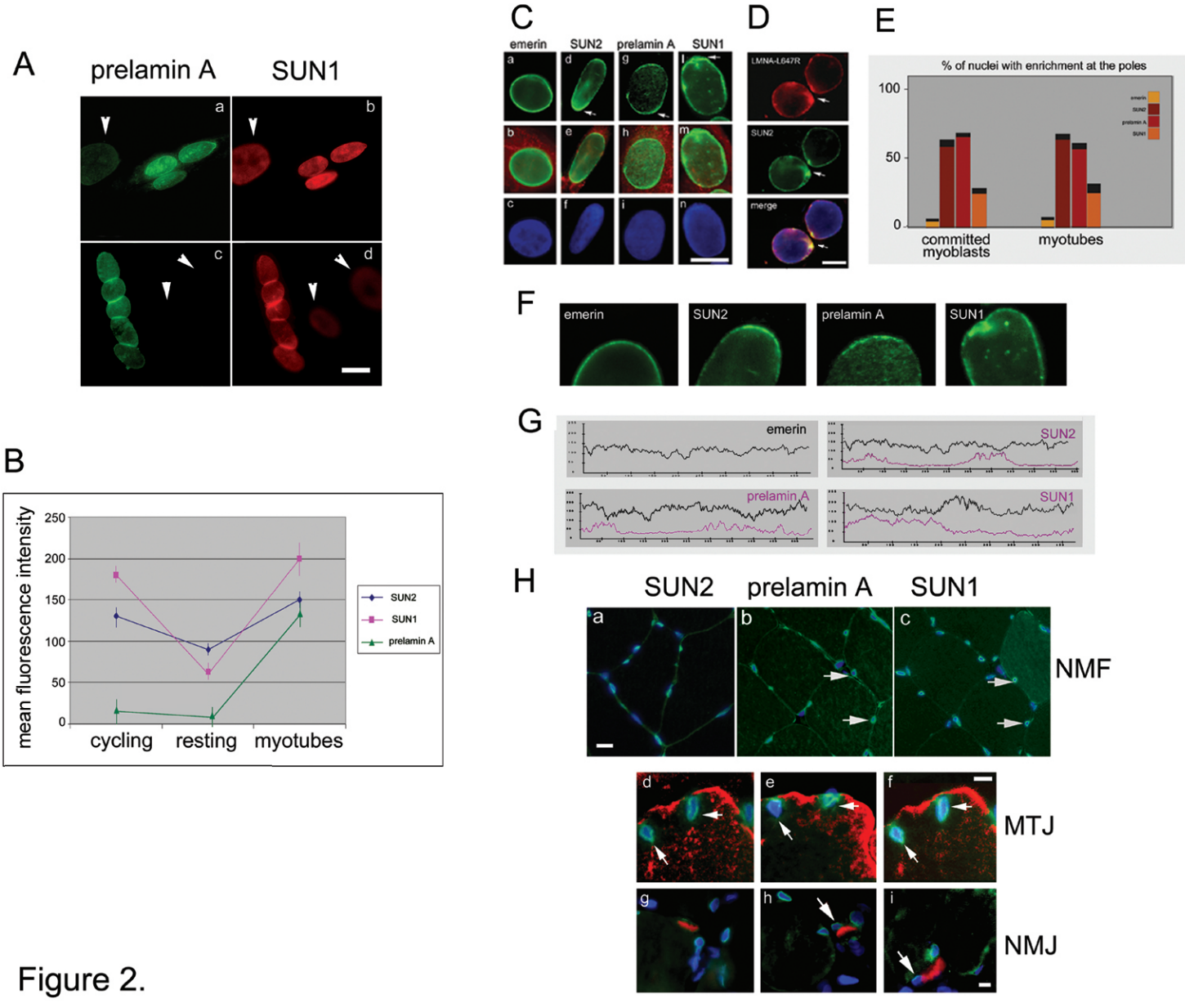
A
prelamin A
SUN1
a
b
c
d
B
mean fluorescence intensity
250
200
150
100
50
0
cycling
resting
myotubes
SUN2
SUN1
prelamin A
C
emerin
SUN2
prelamin A
SUN1
D
LMNA-L647R
SUN2
merge
E
% of nuclei with enrichment at the poles
100
50
0
committed myoblasts
myotubes
F
emerin
SUN2
prelamin A
SUN1
G
emerin
SUN2
prelamin A
SUN1
H
SUN2
prelamin A
SUN1
NMF
MTJ
NMJ

Figure 2.

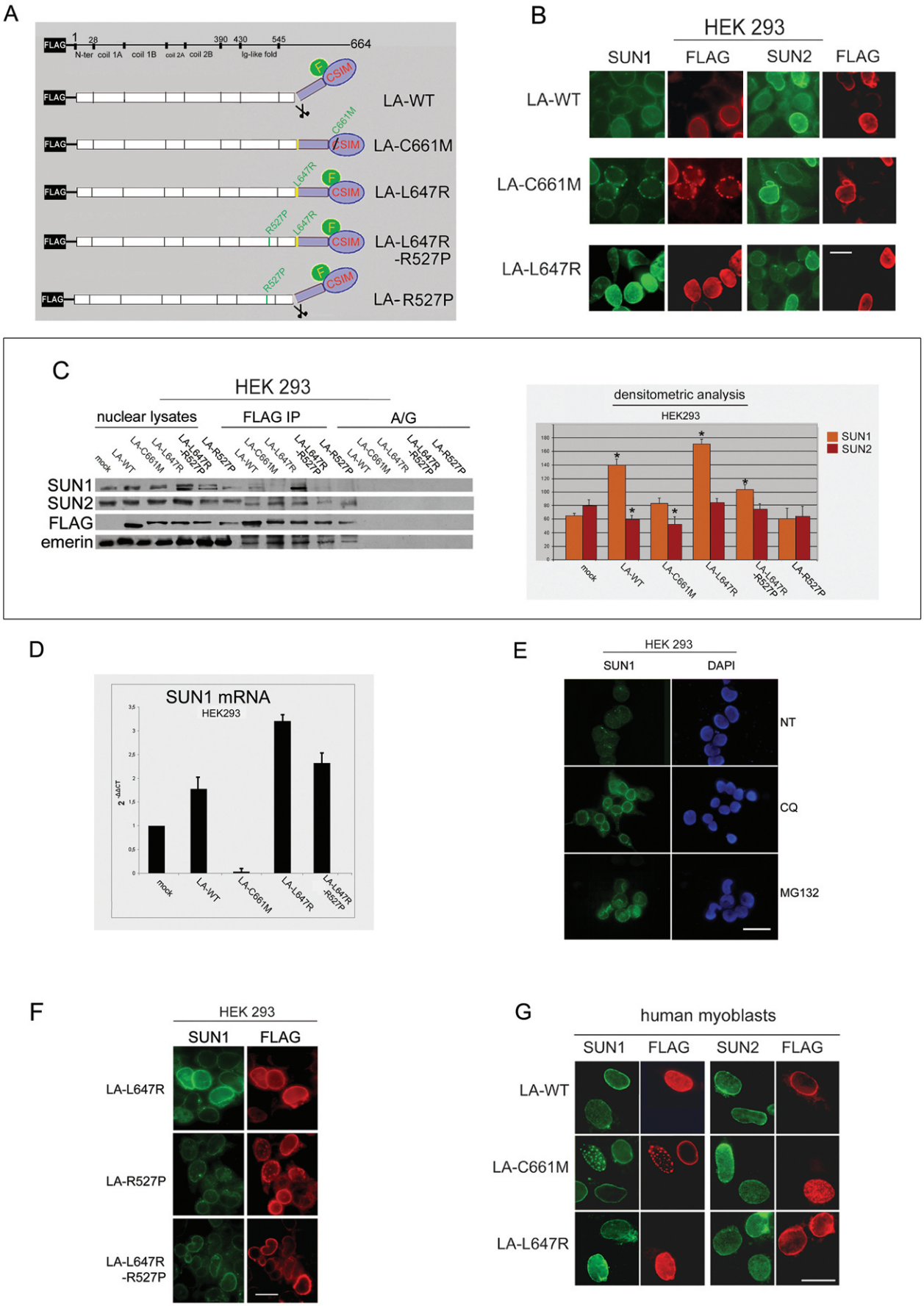
A
FLAG
1
28
390
430
545
664
N-ter
coil 1A
coil 1B
coil 2A
coil 2B
Ig-like fold
F
CSIM
LA-WT
C661M
LA-C661M
L647R
LA-L647R
R527P
LA-L647R -R527P
LA-R527P
B
HEK 293
SUN1
FLAG
SUN2
FLAG
LA-WT
LA-C661M
LA-L647R
C
HEK 293
nuclear lysates
FLAG IP
A/G
mock
LA-WT
LA-C661M
LA-L647R
LA-L647R -R527P
LA-R527P
SUN1
SUN2
FLAG
emerin
densitometric analysis
HEK293
SUN1
SUN2
D
SUN1 mRNA
HEK293
2 ΔΔCT
mock
LA-WT
LA-C661M
LA-L647R
LA-L647R -R527P
E
HEK 293
SUN1
DAPI
NT
CQ
MG132
F
HEK 293
SUN1
FLAG
LA-L647R
LA-R527P
LA-L647R -R527P
G
human myoblasts
SUN1
FLAG
SUN2
FLAG
LA-WT
LA-C661M
LA-L647R

Figure 3.

HUMAN WILD-TYPE MYOBLASTS

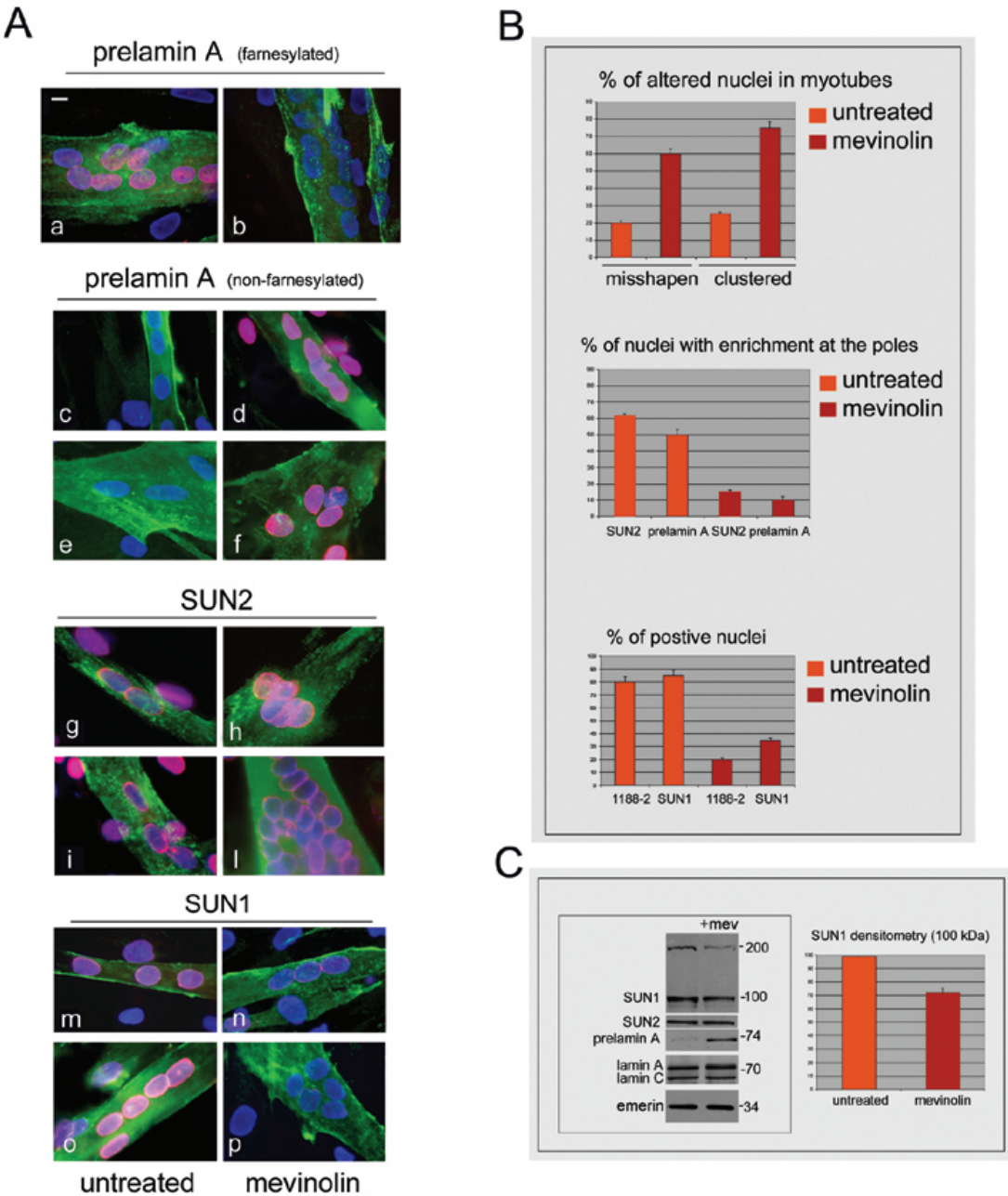

Figure 4.

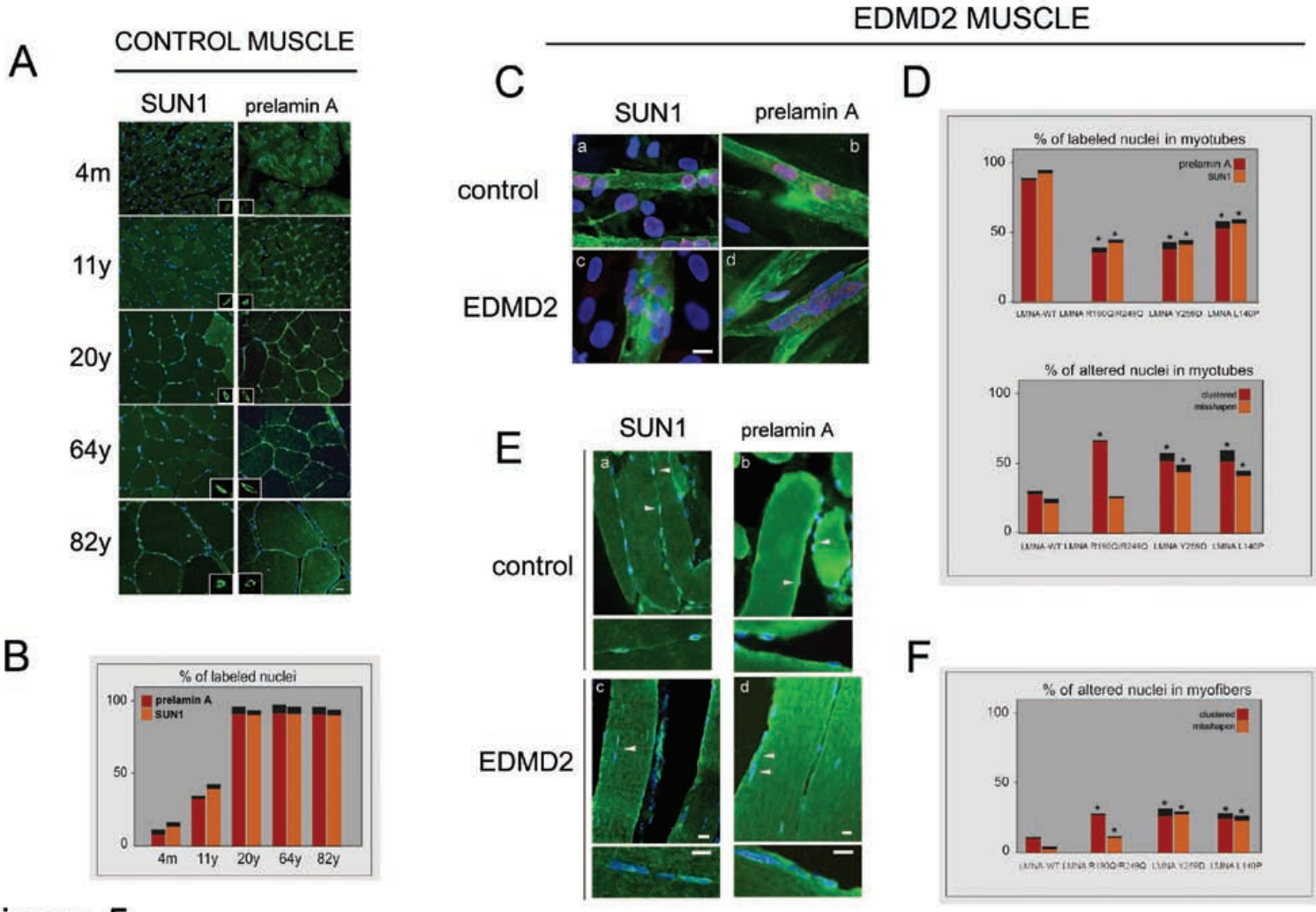
A
CONTROL MUSCLE
SUN1
prelamin A
4m
11y
20y
64y
82y
B
% of labeled nuclei
prelamin A
SUN1
100
50
0
4m
11y
20y
64y
82y
EDMD2 MUSCLE
C
SUN1
prelamin A
control
EDMD2
a
b
c
d
D
% of labeled nuclei in myotubes
prelamin A
SUN1
100
50
0
% of altered nuclei in myotubes
clustered
misshapen
100
50
0
E
SUN1
prelamin A
control
EDMD2
a
b
c
d
F
% of altered nuclei in myofibers
clustered
misshapen
100
50
0

Figure 5.

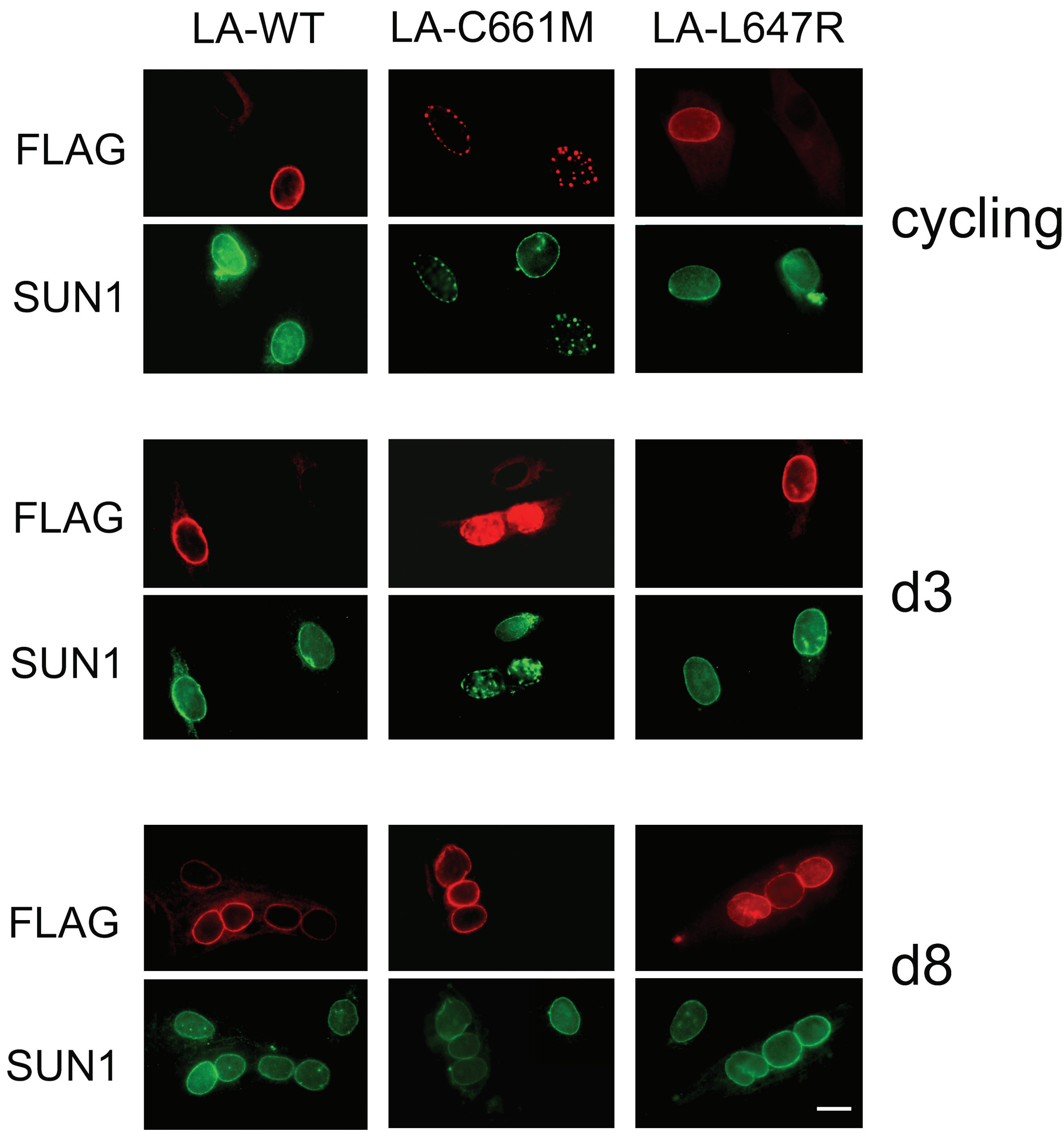

Figure 1.
supplemental material

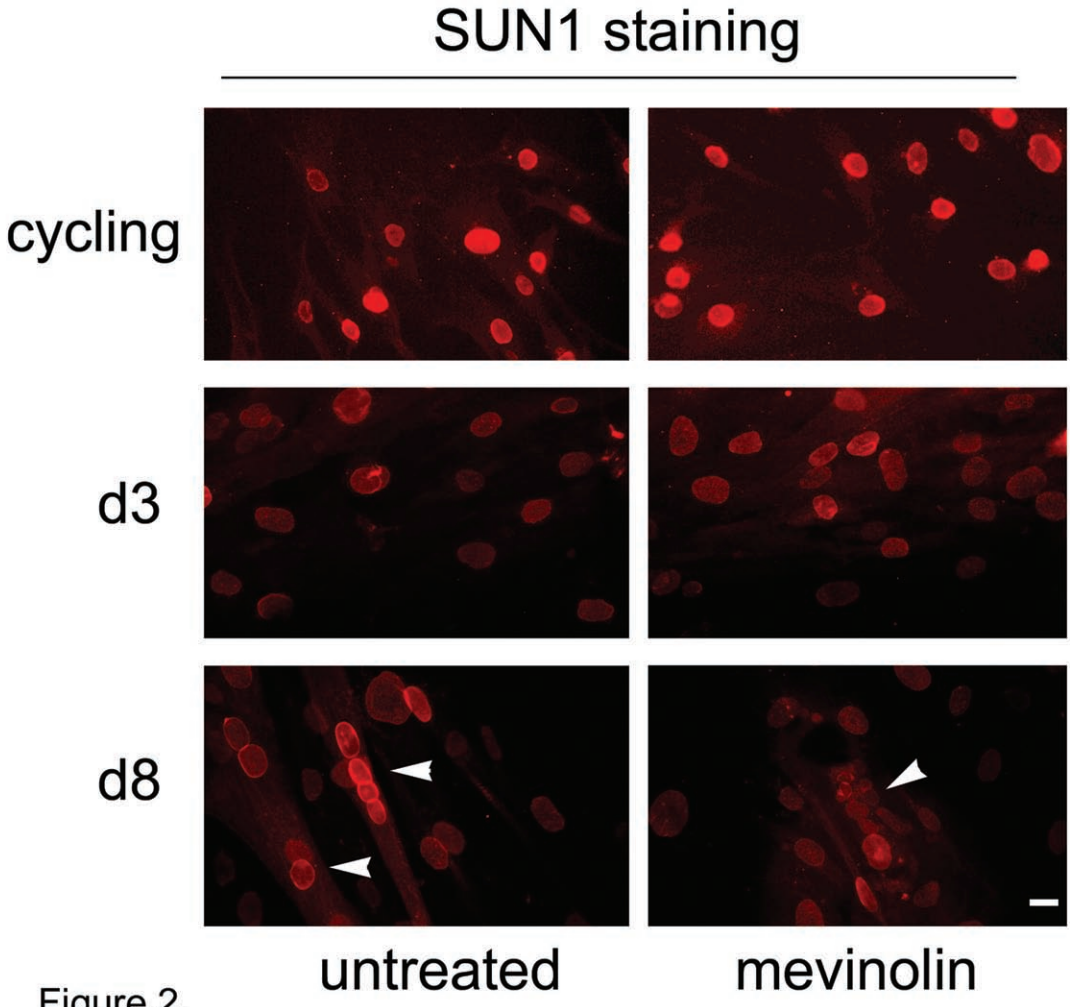

Figure 2.

Supplemental material.

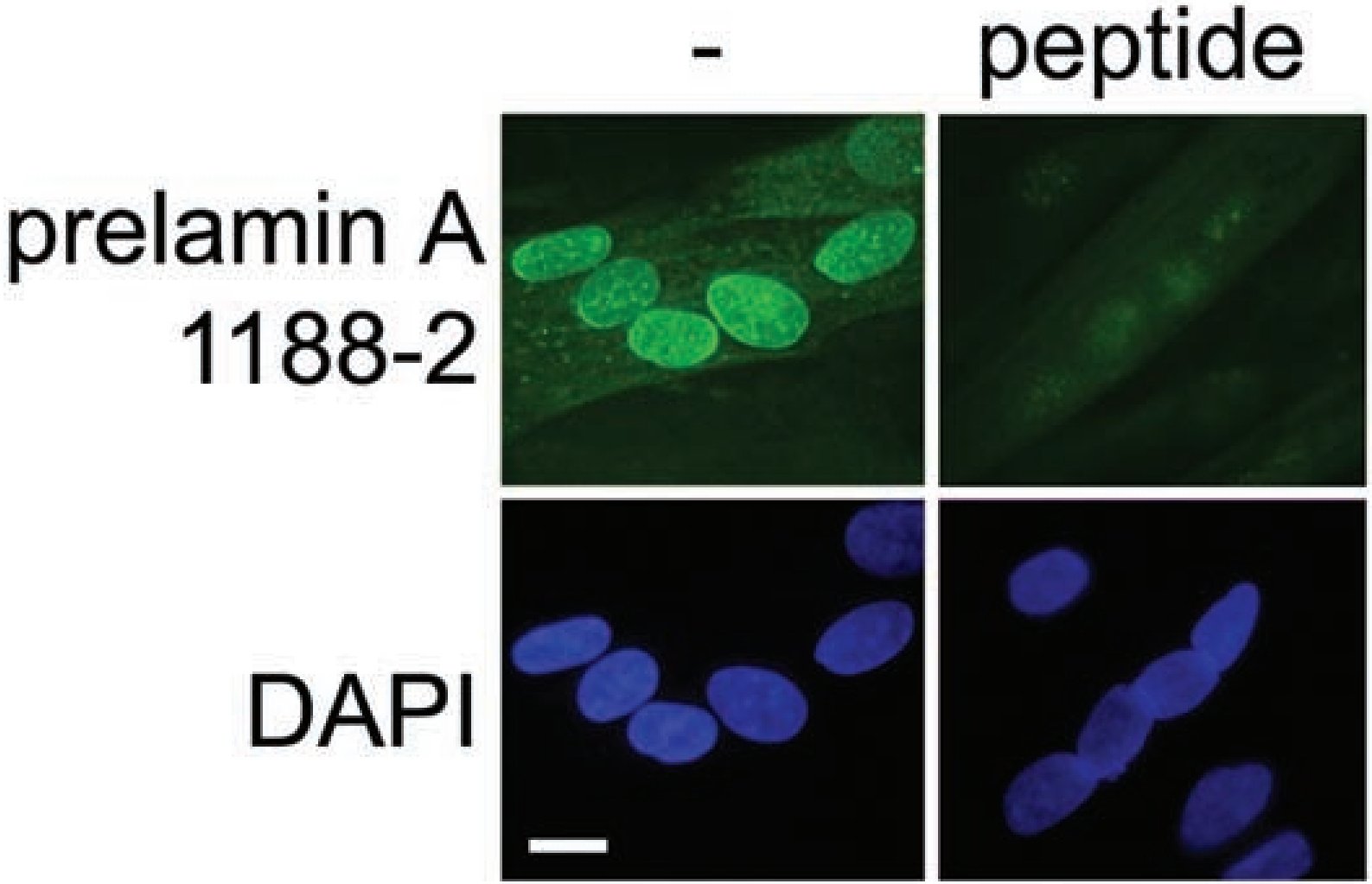

Figure 3.
supplemental material